

Investigation of α clustering with knockout reactions

Kazuki Yoshida,^{1,2,*} Kazuyuki Ogata,^{2,3} and Yoshiko Kanada-En'yo⁴

¹Advanced Science Research Center, Japan Atomic Energy Agency, Tokai, Ibaraki 319-1195, Japan

²Research Center for Nuclear Physics (RCNP), Osaka University, Ibaraki 567-0047, Japan

³Department of Physics, Osaka City University, Osaka 558-8585, Japan

⁴Department of Physics, Kyoto University, Kyoto 606-8502, Japan

(Dated: May 27, 2021)

Background Nuclear clustering has been one of the main interests in nuclear physics. In order to probe the α clustering through reaction observables, α transfer and α knockout reactions have been studied. It is very important to probe the α cluster amplitude at nuclear surface since the α spectroscopic factor is not necessarily a direct measure of the α clustering.

Purpose Our goal is to reveal how the α cluster amplitude is probed through α knockout reactions depending on reaction conditions, e.g., the incident energy.

Method We consider $^{20}\text{Ne}(p, p\alpha)^{16}\text{O}$ and $^{120}\text{Sn}(p, p\alpha)^{116}\text{Cd}$ at 100–400 MeV within the distorted wave impulse approximation (DWIA) framework. We introduce a masking function, which shows how the reaction amplitude in the nuclear interior is suppressed and defines the probed region of the α cluster wave function.

Results It is clearly shown by means of the masking function that the α knockout reaction probes the α cluster amplitude in the nuclear surface region, which is the direct measure of well-developed α cluster states. The incident energy dependence of the masking effect is investigated, using a simplified form of the masking function.

Conclusions The α knockout reaction can probe the α cluster amplitude in the nuclear surface region by choosing proper kinematics owing to the masking effect originated from absorptions of distorting potentials, and is a suitable method to investigate how α cluster states are spatially developed.

PACS numbers: 24.10.Eq, 25.40.-h, 21.60.Gx

I. INTRODUCTION

Cluster states are one of the main interests in nuclear physics. For a recent review, see Ref. [1]. When investigating α cluster states, it should be noted that a large α spectroscopic factor does not necessarily indicate well-developed α cluster states because of the dual nature of the cluster and the shell model [2]. From this point of view, recently the $^{16}\text{O}(^6\text{Li}, d)^{20}\text{Ne}$ α transfer reaction has been studied [3] with a three-body reaction model using a macroscopic cluster wave function, and the reaction was shown to have high sensitivity in the nuclear surface region and suitable to prove the α cluster amplitude there, i.e., spatially developed α cluster states.

An alternative method to the α transfer reaction is the proton-induced α knockout reaction, i.e., $(p, p\alpha)$. In the present study we employ the distorted wave impulse approximation (DWIA) framework, which has been utilized and well established in α knockout reaction studies [4–10] and nucleon knockout reactions [11–16] as well. For a recent review on the (p, pN) reactions, see Ref. [17]. In this paper we examine the peripherality of $^{20}\text{Ne}(p, p\alpha)^{16}\text{O}$ and its incident energy dependence to investigate how the α cluster amplitude in the nuclear surface region is probed through the $^{20}\text{Ne}(p, p\alpha)^{16}\text{O}$ reaction. The $^{120}\text{Sn}(p, p\alpha)^{116}\text{Cd}$ reaction is also investigated in a similar manner.

In Sec. II we describe the DWIA formalism for $(p, p\alpha)$ reactions and also how the cluster wave function is constructed in the present study. The definition of the masking function,

which is the key concept in the present study, is also given. In Sec. III we introduce a general feature of knockout reactions. Then the absorption effect in α knockout reactions due to the distorting potential is discussed in terms of the masking function, which defines the probed region in the $(p, p\alpha)$ reaction. The $^{120}\text{Sn}(p, p\alpha)^{116}\text{Cd}$ reaction is investigated as a case of strong absorption and Coulomb effects. The incident energy dependence of the masking effect is also discussed with introducing a simplified form of the masking function. Finally, a summary is given in Sec. IV.

II. THEORETICAL FRAMEWORK

A. DWIA formalism

In the present study we consider the $^{20}\text{Ne}(p, p\alpha)^{16}\text{O}$ reaction in normal kinematics. The incoming and outgoing protons are labeled as particle 0 and 1, respectively. \mathbf{K}_i , Ω_i , E_i , and T_i denote the momentum (wave number), its solid angle, total and kinetic energy of particle i ($= 0, 1, \alpha$), respectively. All quantities appear below are evaluated in the center-of-mass (c.m.) frame, except those with the superscript L which are in the laboratory (L) frame.

In the DWIA framework, the transition amplitude of $A(p, p\alpha)B$ is given by

$$T_{\mathbf{K}_i}^{nlm} = \left\langle \chi_{1, \mathbf{K}_1}^{(-)} \chi_{\alpha, \mathbf{K}_\alpha}^{(-)} \left| t_{p\alpha} \right| \chi_{0, \mathbf{K}_0}^{(+)} \varphi_\alpha^{nlm} \right\rangle, \quad (1)$$

where χ_{i, \mathbf{K}_i} ($i = 0, 1, \alpha$) are the distorted waves of p -A, p -B, and α -B systems with relative momentum (wave number) \mathbf{K}_i , respectively. The superscripts (+) and (–) are given to

*yoshida.kazuki@jaea.go.jp

specify the outgoing and the incoming boundary conditions of the scattering waves, respectively. The α cluster wave function of the α -B system is denoted by φ_α^{nlm} with n , l , and m being the principal quantum number, the angular momentum, and its third component, respectively. $t_{p\alpha}$ is the effective interaction between p and α , which is the transition interaction in the DWIA framework.

Applying the so-called factorization approximation, or the asymptotic momentum approximation, which has been justified in Ref. [18], Eq. (1) is reduced to

$$T_{\mathbf{K}_i}^{nlm} \approx \tilde{t}_{p\alpha}(\boldsymbol{\kappa}', \boldsymbol{\kappa}) \int d\mathbf{R} F_{\mathbf{K}_i}(\mathbf{R}) \varphi_\alpha^{nlm}(\mathbf{R}), \quad (2)$$

where $\boldsymbol{\kappa}$ ($\boldsymbol{\kappa}'$) is the p - α relative momentum in the initial (final) state. $\tilde{t}_{p\alpha}$ and $F_{\mathbf{K}_i}(\mathbf{R})$ are defined by

$$\tilde{t}_{p\alpha}(\boldsymbol{\kappa}', \boldsymbol{\kappa}) \equiv \int d\mathbf{s} e^{-i\boldsymbol{\kappa}' \cdot \mathbf{s}} t_{p\alpha}(\mathbf{s}) e^{i\boldsymbol{\kappa} \cdot \mathbf{s}}, \quad (3)$$

$$F_{\mathbf{K}_i}(\mathbf{R}) \equiv \chi_{1, \mathbf{K}_1}^{*(-)}(\mathbf{R}) \chi_{\alpha, \mathbf{K}_\alpha}^{*(-)}(\mathbf{R}) \chi_{0, \mathbf{K}_0}^{(+)}(\mathbf{R}) e^{-i\mathbf{K}_0 \cdot \mathbf{R} A_\alpha / A}, \quad (4)$$

where $A_\alpha = 4$ and A is the mass number of the nucleus A . By making the on-the-energy-shell (on-shell) approximation of the final state prescription:

$$\boldsymbol{\kappa} = \boldsymbol{\kappa}' \hat{\boldsymbol{\kappa}}, \quad (5)$$

the matrix element of $t_{p\alpha}$ in Eq. (2) can be related with a free p - α differential cross section as

$$|\tilde{t}_{p\alpha}(\boldsymbol{\kappa}', \boldsymbol{\kappa})|^2 \approx \frac{(2\pi\hbar^2)^2}{\mu_{p\alpha}^2} \frac{d\sigma_{p\alpha}}{d\Omega_{p\alpha}}(\theta_{p\alpha}, T_{p\alpha}), \quad (6)$$

where the p - α scattering angle $\theta_{p\alpha}$ is an angle between $\boldsymbol{\kappa}$ and $\boldsymbol{\kappa}'$, and the scattering energy is defined by $T_{p\alpha} = (\hbar\boldsymbol{\kappa}')^2 / (2\mu_{p\alpha})$ with $\mu_{p\alpha}$ being the reduced mass of the p - α system. The triple differential cross section (TDX) of the $A(p, p\alpha)B$ reaction is then given by

$$\frac{d^3\sigma}{dE_1^L d\Omega_1^L \Omega_2^L} = S_\alpha F_{\text{kin}} C_0 \frac{d\sigma_{p\alpha}}{d\Omega_{p\alpha}}(\theta_{p\alpha}, T_{p\alpha}) \sum_m |\bar{T}_{\mathbf{K}_i}^{nlm}|^2, \quad (7)$$

where S_α is the so-called α spectroscopic factor, and F_{kin} , C_0 , and $\bar{T}_{\mathbf{K}_i}^{nlm}$ are defined by

$$F_{\text{kin}} \equiv J_L \frac{K_1 K_\alpha E_1 E_\alpha}{(\hbar c)^4} \left[1 + \frac{E_\alpha}{E_B} + \frac{E_\alpha}{E_B} \frac{\mathbf{K}_1 \cdot \mathbf{K}_\alpha}{K_\alpha^2} \right]^{-1}, \quad (8)$$

$$C_0 \equiv \frac{E_0}{(\hbar c)^2 K_0} \frac{1}{2l+1} \frac{\hbar^4}{(2\pi)^3 \mu_{p\alpha}^2}, \quad (9)$$

and

$$\bar{T}_{\mathbf{K}_i}^{nlm} \equiv \int d\mathbf{R} F_{\mathbf{K}_i}(\mathbf{R}) \varphi_\alpha^{nlm}(\mathbf{R}) \quad (10)$$

with J_L being the Jacobian from the c.m. frame to the L frame.

The DWIA framework introduced in this section has been validated in Ref. [19] by the benchmark comparison with the transfer-to-the-continuum model [20, 21] and the Faddeev/Alt-Grassberger-Sandhas method [22, 23].

B. α cluster wave function

The α cluster wave function $\varphi_\alpha^{nlm}(\mathbf{R})$ for the α - ^{16}O system is defined as the eigenstate of the Schrödinger equation:

$$\left[-\frac{\hbar^2}{2\mu_\alpha} \nabla_{\mathbf{R}}^2 + V_{\alpha B}(R) \right] \varphi_\alpha^{nlm}(\mathbf{R}) = \varepsilon_\alpha \varphi_\alpha^{nlm}(\mathbf{R}), \quad (11)$$

where μ_α , $V_{\alpha B}$, and ε_α are the reduced mass, the binding potential, and the binding energy of α -B system, respectively.

For the nuclear part of $V_{\alpha B}$, a central Woods-Saxon shape with the radius parameter r_0 and the diffuseness parameter a_0 is adopted:

$$f_{\text{WS}}(R) = \frac{1}{1 + \exp\left(\frac{R - r_0}{a_0}\right)}. \quad (12)$$

The numerical input for r_0 , a_0 and ε_α are given in Sec. III A. Since $V_{\alpha B}$ is a central potential, $\varphi_\alpha^{nlm}(\mathbf{R})$ can be simply separated into the radial and the angular part as

$$\varphi_\alpha^{nlm}(\mathbf{R}) = \phi_\alpha^{nl}(R) Y_{lm}(\Omega), \quad (13)$$

where $\phi_\alpha^{nl}(R)$, Y_{lm} , and Ω are the radial part of $\varphi_\alpha^{nlm}(\mathbf{R})$, the spherical harmonics, and the solid angle of \mathbf{R} , respectively.

C. Masking function

Since the square modulus of Eq. (10) is proportional to the knockout cross section, it should be worth investigating the property of the integrand in the right-hand side of Eq. (10) to reveal a contribution of φ_α^{nlm} to the knockout cross section. Here we define the masking function

$$D_{lm}(R) \equiv \frac{1}{\sqrt{4\pi}} \int d\Omega F_{\mathbf{K}_i}(\mathbf{R}) Y_{lm}(\Omega) \quad (14)$$

so that $\bar{T}_{\mathbf{K}_i}^{nlm}$ is given by

$$\bar{T}_{\mathbf{K}_i}^{nlm} = \sqrt{4\pi} \int dR R^2 D_{lm}(R) \phi_\alpha^{nl}(R). \quad (15)$$

Therefore the masking function $D_{lm}(R)$ is a weighting function which determines the radial contribution of $\phi_\alpha^{nl}(R)$ to the knockout reaction amplitude.

If the nucleus B can be treated as a spectator, the total momentum of the p - α system is approximately conserved;

$$\mathbf{k}_\alpha \approx \mathbf{q} \equiv \mathbf{K}_1 + \mathbf{K}_\alpha - \left(1 - \frac{A_\alpha}{A}\right) \mathbf{K}_0, \quad (16)$$

where \mathbf{q} is the so-called missing momentum and \mathbf{k}_α is the momentum of the α cluster in the nucleus A in the initial state. It can be shown that \mathbf{k}_α is actually the momentum $-\mathbf{K}_B^L$. Once all distorting potentials are switched off, i.e., the plane wave impulse approximation (PWIA) is adopted, $\bar{T}_{\mathbf{K}_i}^{nlm}$ turns out to be the Fourier transform of the α cluster wave function,

$$\bar{T}_{\mathbf{K}_i}^{nlm} \approx \int d\mathbf{R} e^{-i\mathbf{k}_\alpha \cdot \mathbf{R}} \phi_\alpha^{nl}(\mathbf{R}). \quad (17)$$

The masking function $D_{lm}(R)$ is normalized to unity when an $l = 0$ cluster wave function is considered in PWIA, as discussed in Sec. III B.

III. RESULTS AND DISCUSSION

A. Numerical inputs

In the calculation of $^{20}\text{Ne}(p, p\alpha)^{16}\text{O}$, $n = 4$, and $l = 0$ are assumed for the α cluster orbital. For the binding potential $V_{\alpha\text{B}}(R) = V_0 f_{\text{WS}}(R)$, the radius parameter $r_0 = 1.25 \times 16^{1/3}$ fm and the diffuseness parameter $a_0 = 0.76$ fm are employed. These parameters are fixed to describe the behavior of the microscopic cluster model wave function in the tail region [3]. The depth parameter V_0 is determined so as to reproduce the α separation energy of 4.73 MeV. In Fig. 1 we show the obtained $\phi_\alpha^{40}(R)$ by solving Eq. (11). The solid, dashed, and dotted lines are $\phi_\alpha^{40}(R)$, $R\phi_\alpha^{40}(R)$, and

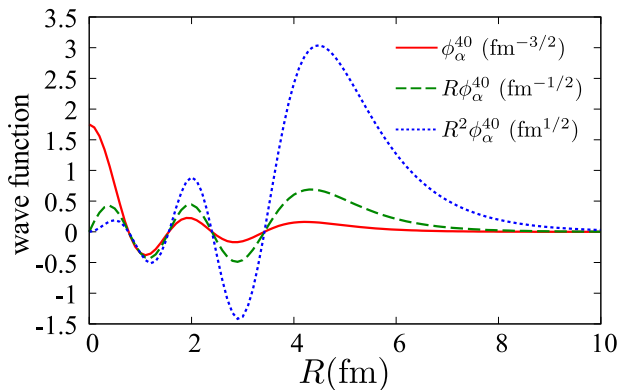


FIG. 1: α cluster wave function obtained by solving Eq. (11). The solid, dashed, and dotted lines correspond to $\phi_\alpha^{40}(R)$, $R\phi_\alpha^{40}(R)$, and $R^2\phi_\alpha^{40}(R)$, respectively. The dashed line is equivalent to the PM1 in Fig. 3 of Ref. [3].

$R^2\phi_\alpha^{40}(R)$, respectively. The dashed line is equivalent to the PM1 in Fig. 3 of Ref. [3]. The dotted line in Fig. 1 shows a cluster wave function multiplied by R^2 , which will be helpful in the following discussion because R^2 appears as a weight on $\phi_\alpha^{40}(R)$ in the transition matrix, as shown in Eq. (15).

For the optical potentials of the incoming and outgoing protons, the global optical potential by Koning and Delaroche [24] is employed, and for the α - ^{16}O potential in the final state, the parameter set by Nolte, *et al.* [25] is employed. For calculating the p - α scattering cross section, the microscopic single folding model [26] with a phenomenological α density and the Melbourne nucleon-nucleon (NN) g -matrix interaction [27] is adopted.

B. $^{20}\text{Ne}(p, p\alpha)^{16}\text{O}$ reaction

In Fig. 2 we show the TDX of $^{20}\text{Ne}(p, p\alpha)^{16}\text{O}$ at 392 MeV as a function of the recoil momentum p_R defined by

$$p_R = \hbar K_B^L \frac{K_{Bz}^L}{|K_{Bz}^L|}, \quad (18)$$

where K_{Bz}^L is the z -component of \mathbf{K}_B^L following the Madison convention. The kinematics are fixed to be $T_1 = 352$ MeV, $\theta_1^L = 32.5^\circ$, and $T_\alpha(\theta_\alpha)$ varies 31–35 MeV (27 – 108°). The azimuthal angles ϕ_{K_1} and ϕ_{K_2} are fixed at 0 and π , respectively, i.e., the scattered particles are in a coplanar. The TDX has a peak at $p_R \sim 0$ MeV/c when $l = 0$, since p_R corresponds to the momentum of α in the initial state in quasifree knockout reactions.

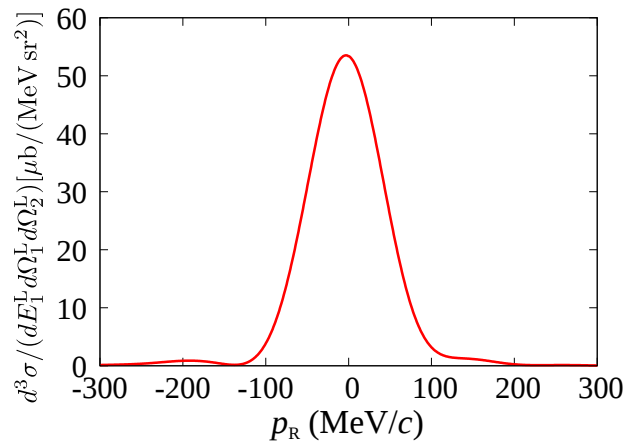


FIG. 2: TDX of $^{20}\text{Ne}(p, p\alpha)^{16}\text{O}$ at 392 MeV as a function of the recoil momentum.

In Fig. 3 we investigate the masking function $D_{00}(R)$ and the radial reaction amplitude $I(R)$ at $p_R = 0$ MeV/c. The latter is defined by

$$I(R) \equiv R^2 |D_{00}(R)| \phi_\alpha^{40}(R), \quad (19)$$

which corresponds to the integrand of R in Eq. (15). As shown by the solid line in Fig. 3(a), $|D_{00}(R)|$ is enough small in the nuclear interior region to suppress contribution of the α amplitude in this region to $I(R)$ because of the absorption effect of the distorting potentials. The result without the Coulomb interaction V_c (dashed line in Fig. 3(a)) approaches to unity in the asymptotic region because all the nuclear potentials are absent there and $F_{K_i}(\mathbf{R}) = 1$ when $q = 0$; see Eqs. (4) and (16). On the other hand, the result of DWIA including V_c (solid line) never reaches to unity even in the asymptotic region. This is because $F_{K_i}(\mathbf{R})$ suffers from the long-range nature of the Coulomb interaction. Even if the asymptotic momenta of the three particles satisfy $\mathbf{q} = 0$, finite values of the Coulomb phase shifts of the scattering waves make $|D_{00}(R)|$ deviate from unity when R is finite.

Figure 3(b) shows $I(R)$ defined by Eq. (19). One sees that $I(R)$ of DWIA (solid line) is strongly suppressed in the

interior region, compared with that of PWIA divided by 3 (dotted line). The result of DWIA without Coulomb interactions (dashed line) agrees well with that of DWIA (solid line), since the cluster wave function has an amplitude for $R \lesssim 8$ fm, where $|D_{00}(R)|$ with and without Coulomb interactions agrees well each other. Therefore the deviation of the solid line in Fig. 3(a) from unity due to Coulomb interactions makes no difference in understanding the property of $D_{00}(R)$. This allows one to make further simplification of $D_{00}(R)$ as discussed in Sec. III D.

The masking effect on the cluster wave function due to nuclear distorting potentials can be a great advantage of $(p, p\alpha)$ reactions for probing α cluster states. A large $(p, p\alpha)$ cross section corresponds to a large cluster amplitude around the nuclear surface, which indicates an existence of well-developed α cluster states in a nucleus. It should be noted that in the nuclear interior, the NN antisymmetrization plays a significant role, which makes even the definition of the α cluster unclear. Because of the masking effect, $(p, p\alpha)$ reactions automatically avoid such an unclear region and focus the nuclear surface. In consequence of this, one can conclude that what is determined by $(p, p\alpha)$ is not an α spectroscopic factor S_α but the surface

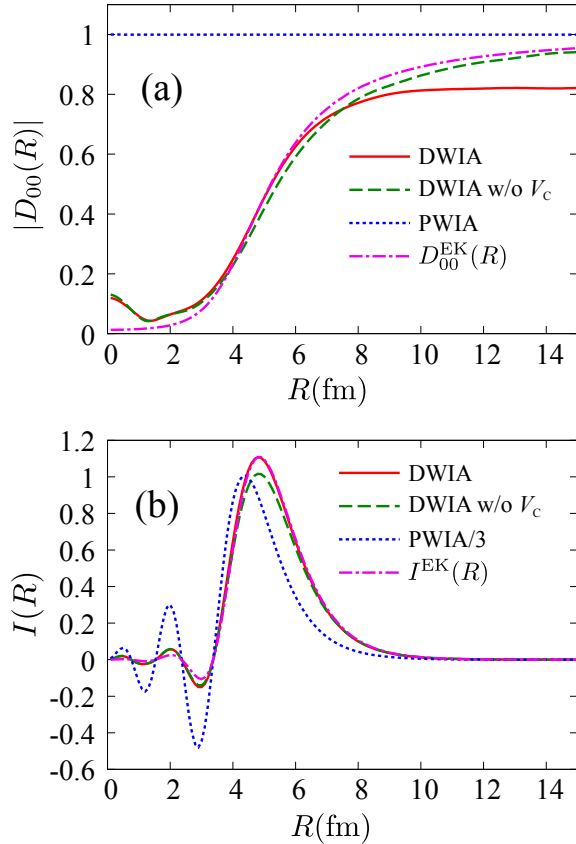


FIG. 3: (a) Masking function $|D_{00}(R)|$ defined by Eq. (15). The solid, dashed, and dotted lines represent $|D_{00}(R)|$ of DWIA, DWIA without Coulomb interactions, and PWIA, respectively. The dot-dashed line shows the eikonal-masking function $|D_{00}^{\text{EK}}(R)|$ discussed in Sec. III D. (b) Same as (a) but $I(R)$ and that with the eikonal approximation $I^{\text{EK}}(R)$.

amplitude of the α distribution, and the latter is the measure of the α clustering.

C. Coulomb effect in $^{120}\text{Sn}(p, p\alpha)^{116}\text{Cd}$ reaction

As shown in Fig. 3 (a), long-ranged Coulomb interactions prohibit the masking function from reaching unity, even if the kinematics of the knockout process is fixed so as to satisfy $q = 0$. This effect becomes significant when the charge of the target nucleus is large. In this point of view, we investigate the peripheral property of the $^{120}\text{Sn}(p, p\alpha)^{116}\text{Cd}$ reaction at 392 MeV and the masking function as well. The α cluster wave function is constructed in the same method as mentioned above but with $r_0 = 1.25 \times 116^{1/3}$ fm and $\varepsilon_\alpha = -4.81$ MeV. The three-body kinematics are chosen to be $T_1 = 328$ MeV, $\theta_1^L = 43.2^\circ$, $T_\alpha = 51$ MeV, and $\theta_\alpha = 61^\circ$, which satisfies $q = 0$.

In Fig. 4 $|D_{00}(R)|$ and $I(R)$ of $^{120}\text{Sn}(p, p\alpha)^{116}\text{Cd}$ are shown in the same manner as in Fig. 3. The obtained masking

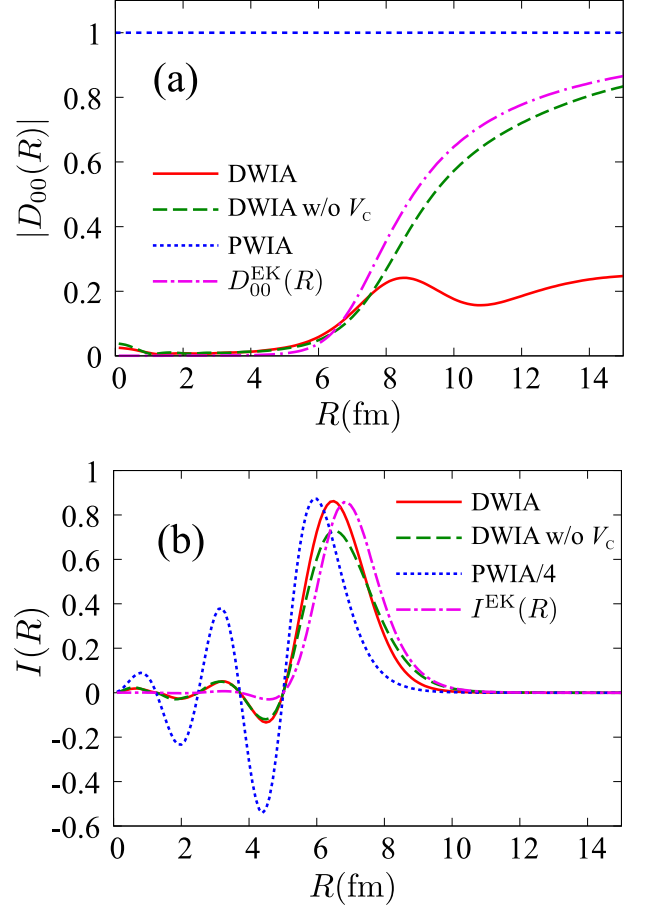


FIG. 4: The same as Fig. 3 but for $^{120}\text{Sn}(p, p\alpha)^{116}\text{Cd}$ reaction.

function for this system (the solid line in Fig. 4 (a)) is only 0.2–0.3 even in the asymptotic region by the Coulomb interactions. On the other hand, $D_{00}(R)$ without V_C (the dashed line) tends to approach unity, as well as the eikonal masking

function $D_{00}^{\text{EK}}(R)$ (dot-dashed line). This peculiar behavior of $D_{00}(R)$ at larger R , however, causes no serious problem, because the α cluster wave function is sufficiently damped in that region. Consequently, the dashed line and the dot-dashed line agree quite well with the solid line in Fig. 4 (b) indicating that $I(R)$ can be approximately simulated by analyses of the masking function without Coulomb interactions and also the eikonal masking function. It turns out that only the α amplitude at the nuclear surface can be safely probed by α knockout reactions even in the case of heavy-mass targets.

D. Incident energy dependence of masking function

It is important to clarify how the aforementioned property of the masking function depends on the incident energy. For this purpose, a more simplified functional form of the masking function is preferable. We thus rely on the eikonal approximation and use the following form:

$$D_{00}^{\text{EK}}(R) \equiv \frac{1}{4\pi} \int d\Omega \exp \left[-C_{\text{abs}} \int_{-\infty}^{\infty} dz f_{\text{WS}}(\mathbf{R}) \right] e^{-i\mathbf{q}\cdot\mathbf{R}}, \quad (20)$$

which is designated eikonal masking function. C_{abs} represents the total strength of the absorption caused by the distorting potentials of particles 0–2, and is determined so that the peak height of

$$I^{\text{EK}}(R) \equiv R^2 |D_{00}^{\text{EK}}(R)| \phi_{\alpha}^{40}(R) \quad (21)$$

reproduces that of $I(R)$. Thus, one can characterize the masking function $D_{00}(R)$ by just one parameter C_{abs} . In a naïve interpretation, C_{abs} is related to the mean free path (MFP) λ through $1/\lambda = 2C_{\text{abs}}f_{\text{WS}}(R)$.

The dot-dashed lines in Fig. 3(a) and 3(b) represent $|D_{00}^{\text{EK}}(R)|$ and $I^{\text{EK}}(R)$, respectively; C_{abs} is taken to be 0.69 fm^{-1} . One sees in Fig. 3(a) that the dot-dashed line agrees well with the solid line for $4 \lesssim R \lesssim 6 \text{ fm}$ and slightly deviates from it for larger R . This asymptotics of the dot-dashed line can be understood as a result of absence of Coulomb interactions in Eq. (20). Nevertheless, as shown in Fig. 3(b), the dot-dashed line, $I^{\text{EK}}(R)$, agrees well with the solid line for $R \gtrsim 4 \text{ fm}$, in which the integrand $I(R)$ has a meaningful amplitude. This indicates that Eq. (20) is sufficient to describe the property of the masking function that is relevant to the $(p, p\alpha)$ reaction considered. It should be noted that the small but finite difference between the solid and dot-dashed lines in Fig. 3(a) for $R \gtrsim 6 \text{ fm}$ appears also in Fig. 3(b); for instance, the difference is about 6% at 8 fm. We then discuss the incident energy T_0 dependence of C_{abs} , which is shown in Fig. 5. At each T_0 , the scattering energies and angles of particle 1 and α are chosen so as to satisfy $p_R = 0 \text{ MeV}/c$. It is found that the T_0 dependence of C_{abs} is weak above 200 MeV, where the quasi-free (impulse) picture of the knockout reaction is valid. On the other hand, below 200 MeV, C_{abs} increases rather rapidly as T_0 decreases. This behavior can be understood by the fact that the MFP's of low

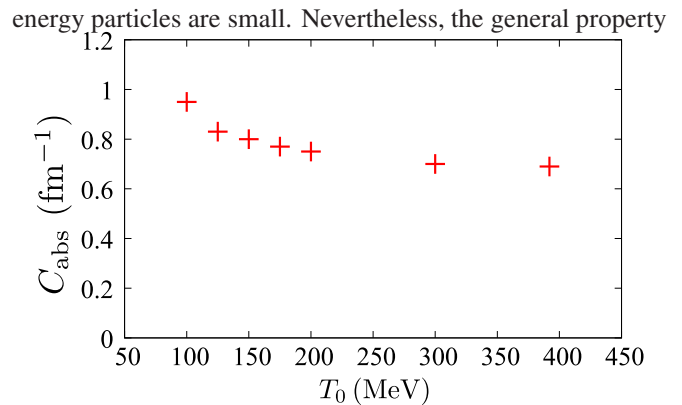


FIG. 5: Incident energy T_0 dependence of C_{abs} .

of the masking function and the peripherality of the reaction are found to be robust for T_0 shown in Fig. 5.

IV. SUMMARY

$^{20}\text{Ne}(p, p\alpha)^{16}\text{O}$ reactions at 100–392 MeV were investigated within the distorted wave impulse approximation framework. We have introduced the masking function, which describes the absorption effect due to distorting potentials of the incident p and also the emitted p and α and suppresses the α amplitude contribution in the interior region to the α knockout cross section. Through the analyses on the masking functions of the reactions, it is clearly shown that α knockout reactions are peripheral and suitable for probing the α cluster amplitude in the nuclear surface, which is regarded as a direct measure of spatially developed α cluster states.

As a case of strong Coulomb interactions, the $^{120}\text{Sn}(p, p\alpha)^{116}\text{Cd}$ reaction at 392 MeV has been investigated. It is shown that in this case the masking function has a nontrivial behavior at larger distance due to Coulomb interactions. Nevertheless, this does not cause any problem because the overlap between the masking function and the cluster amplitude in that region is negligibly small.

To investigate the incident energy T_0 dependence of the masking function, we introduce a simplified functional that is characterized by only one parameter C_{abs} . It was found that C_{abs} depends weakly on T_0 for 200–400 MeV. At lower energies, C_{abs} increases rather rapidly, corresponding to stronger absorption. However, the feature of the masking function turned out to be robust down to 100 MeV.

ACKNOWLEDGMENTS

A part of the computation was carried out with the computer facilities at the Research Center for Nuclear Physics, Osaka University. This work was supported in part by Grants-in-Aid of the Japan Society for the Promotion of Science (Grants No. JP16K05352, JP15J01392, and No. JP26400270).

-
- [1] H. Horiuchi, K. Ikeda, and K. Kato, *Prog. Theor. Phys. Supplement* **192**, 1 (2012).
- [2] B. F. Bayman and A. Bohr, *Nucl. Phys.* **9**, 596 (1958/59).
- [3] T. Fukui, Y. Taniguchi, T. Suhara, Y. Kanada-En'yo, and K. Ogata, *Phys. Rev. C* **93**, 034606 (2016).
- [4] T. A. Carey, P. G. Roos, N. S. Chant, A. Nadasen, and H. L. Chen, *Phys. Rev. C* **29**, 1273 (1984).
- [5] J. Mabiála, A. A. Cowley, S. V. Förtsch, E. Z. Buthelezi, R. Neveling, F. D. Smit, G. F. Steyn, and J. J. Van Zyl, *Phys. Rev. C* **79**, 054612 (2009).
- [6] P. G. Roos, N. S. Chant, A. A. Cowley, D. A. Goldberg, H. D. Holmgren, and R. Woody, III, *Phys. Rev. C* **15**, 69 (1977).
- [7] A. Nadasen, N. S. Chant, P. G. Roos, T. A. Carey, R. Cowen, C. Samanta, and J. Wesick *Phys. Rev. C* **22**, 1394 (1980).
- [8] A. Nadasen, P. G. Roos, N. S. Chant, C. C. Chang, G. Ciangaru, H. F. Breuer, J. Wesick, and E. Norbeck, *Phys. Rev. C* **40**, 1130 (1989).
- [9] C. W. Wang, P. G. Roos, N. S. Chant, G. Ciangaru, F. Khazaie, D. J. Mack, A. Nadasen, S. J. Mills, R. E. Warner, E. Norbeck, F. D. Becchetti, J. W. Janecke, and P. M. Lister, *Phys. Rev. C* **31**, 1662 (1985).
- [10] T. Yoshimura, A. Okihana, R. E. Warner, N. S. Chant, P. G. Roos, C. Samanta, S. Kakigi, N. Koori, M. Fujiwara, N. Matsuoka, K. Tamura, E. Kubo, and K. Ushiro, *Nucl. Phys. A* **641**, 3 (1988).
- [11] C. Samanta, N. S. Chant, P. G. Roos, A. Nadasen, J. Wesick, and A. A. Cowley, *Phys. Rev. C* **34**, 1610 (1986).
- [12] N. S. Chant and P. G. Roos, *Phys. Rev. C* **15**, 57 (1977).
- [13] C. Samanta, N. S. Chant, P. G. Roos, A. Nadasen, and A. A. Cowley, *Phys. Rev. C* **35**, 333 (1987).
- [14] G. Jacob and Th. A. J. Maris, *Rev. Mod. Phys.* **38**, 121 (1966).
- [15] G. Jacob and Th. A. J. Maris, *Rev. Mod. Phys.* **45**, 6 (1973).
- [16] P. Kitching, W. J. McDonald, Th. A. J. Maris, and C. A. Z. Vasconcellos, *Adv. Phys. Part. Nuclei* **15**, 43 (1985).
- [17] T. Wakasa, K. Ogata, and T. Noro, *Progress in Particle and Nuclear Physics* **96**, 32 (2017).
- [18] K. Yoshida, K. Minomo, and K. Ogata, *Phys. Rev. C* **94** 044604 (2016).
- [19] K. Yoshida, M. Gómez-Ramos, K. Ogata, and A. M. Moro, *Phys. Rev. C* **97**, 024608 (2018).
- [20] A. M. Moro, *Phys. Rev. C* **92**, 044605 (2015).
- [21] M. Gómez-Ramos J. Casal, and A. M. Moro, *Phys. Lett. B* **772** 115 (2017).
- [22] L. D. Faddeev, *Zh. Eksp. Teor. Fiz.* **39**, 1459 (1960) [*Sov. Phys. JETP* **12**, 1014 (1961)].
- [23] E. O. Alt, P. Grassberger, and W. Sandhas, *Nucl. Phys. B* **2**, 167 (1967).
- [24] A. J. Koning and J. P. Delaroche, *Nucl. Phys. A* **713** 231 (2003).
- [25] M. Nolte, H. Machner, and J. Bojowald, *Phys. Rev. C* **36**, 1312 (1987).
- [26] M. Toyokawa, K. Minomo, and M. Yahiro, *Phys. Rev. C* **88**, 054602 (2013).
- [27] K. Amos, P. J. Dortmans, H. V. von Geramb, S. Karataglidis, and J. Raynal, *Adv. Nucl. Phys.* **25**, 276 (2000).